Phase diagram of ultracold strongly coupled plasmas

2006 J. Phys. A: Math. Gen. 39 4579

(http://iopscience.iop.org/0305-4470/39/17/S42)

INSTITUTE OF PHYSICS PUBLISHING JOURNAL OF PHYSICS A: MATHEMATICAL AND GENERAL

J. Phys. A: Math. Gen. **39** (2006) 4579–4585 doi:10.1088/0305-4470/39/17/S42

Phase diagram of ultracold strongly coupled plasmas

Genri E Norman

Institute for High Energy Density, Izhorskay 13/19, Moscow 125412, Russia

E-mail: norman@ihed.ras.ru

Received 21 October 2005, in final form 22 December 2005
Published 7 April 2006
Online at stacks.iop.org/JPhysA/39/4579

Abstract

The results of recent experiments and simulation for ultracold plasmas are related to the criterion of the thermodynamic stability. Different approaches for the equation of state of strongly coupled plasmas are used: second virial coefficient, electrolyte-like and van der Waals-like approximations. Three areas of ultracold plasma parameters are distinguished: thermodynamically stable, labile and metastable.

PACS numbers: 52.27.Gr, 64.60.My, 71.10.Hf

1. Introduction

Recent experiments [1–4] opened a new regime of ultracold neutral plasmas with temperatures as low as 1 K. The experiments have so far used xenon [1–4] and strontium [4]. Moderately low temperatures about 10^2 K were obtained experimentally for caesium in [5] for the plasma state and in [6, 7] for so-called Rydberg matter [8–12], which in fact was closely related to the ultracold neutral plasmas. Several recent papers addressed simulation and theory of ultracold neutral plasmas [13–18] and Rydberg matter [19, 20].

Plasma parameters achieved in the experiments [1–7] and simulated in [13–15, 19] had included the area where the number N_D of electrons in the Debye sphere became less than unity. It meant that the plasmas were nonideal (strongly coupled). However the plasmas remained non-degenerate. Nonideal non-degenerate plasmas should have been analysed with respect to the thermodynamic stability. The concept of *thermodynamical instability* of nonideal plasmas was developed in [21, 22]. According to that idea, the instability could occur as a result of the competition between the classical long-range Coulomb attraction of charges (the attraction prevails with respect to the Coulomb repulsion) and their quantum repulsion at small distances. The situation was quite similar to the van der Waals equation, for which the thermodynamical instability could occur as a result of the competition between the long-range attraction of molecules and their short-range repulsion.

If one extrapolated the approach [21, 22] to ultracold neutral plasmas the thermodynamic instability would have been discovered for some parameters studied. However the possibility of

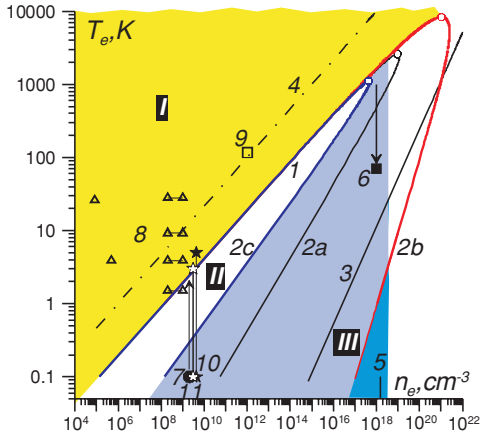

Figure 1. T–n_e diagram. *Theoretical estimates*: 1—$\pi^{1/2}\gamma^{3/2} = 2$, 2a—(3), 2b—(7), 2c—(9), 3—border of degeneracy, 4—$N_D = 1$, 5—the conditional right border of the metastability area for $\tau = 1$ s. *Experimental points*: 6—[6, 7], 7—[1], 8—[2], 9—[5]. *Simulation*: 10—[13], 11—[14, 15].

the loss of thermodynamic stability when one proceeded to nonideal non-degenerate ultracold neutral plasmas was not taken into account in the discussions of experiment, theory and simulation results in [1–5, 13–19]. The problem is considered in the present communication.

2. T–n_e diagram

Lines 1 and 2 are two of the most principal lines in figure 1. The areas of stable and/or metastable states of nonideal plasma are bounded by the condition of thermodynamic stability, or the line $(\partial P/\partial V)_T = 0$, where P is the pressure, V is the volume [21, 22]. In fact there are two such lines in figure 1: line 1 where plasma loses thermodynamic stability, $(\partial P/\partial V)_T > 0$ below line 1, and line 2, where nonideal plasma has its thermodynamic stability restored, $(\partial P/\partial V)_T < 0$ below line 2. The value of nonideality parameter $\gamma = e^2(2n_e)^{1/3}/kT_e \approx 1$ on line 1. The condition $\gamma \gtrsim 1$ corresponds to the loss of thermodynamic stability below the critical temperature T_c in almost all the approaches for plasma thermodynamics [22–24]. The opinions are much more diverse concerning the restoration of the thermodynamic stability due to quantum repulsion [22–24]. So the position of line 2 is more uncertain than that of line 1. To illustrate the possible scatter of line 2 position and T_c estimations we use three approaches (lines 2a, 2b and 2c in figure 1).

2.1. Virial expansion

The expansion for plasmas is obtained in [25]. $F_1 = F_0 - \Delta F_1$ for the free energy of electrons and single-charged ions, where F_0 is the free energy of ideal gas, and the virial contribution is

$$\Delta F_1 = F_{DH}(1 - 0.75C\lambda\kappa) \tag{1}$$

where $F_{DH} = (2/3)\pi^{1/2}e^3N^{3/2}(k_BTV)^{-1/2}$ is the Debye–Hückel free energy of a classical system of charged particles, $N = 2N_e$—the number of electrons and ions in the volume V, $N_e = n_eV$, $\lambda = h(3k_BTm)^{-1/2}$—the de Broglie electron thermal wavelength, κ—the inverse Debye radius, $C \approx 0.1$. The term $0.75C\lambda\kappa$ takes into account the quantum repulsion between charges. The multiplier $1 - 0.75C\lambda\kappa$ reduces the effective attraction which is given

by F_{DH}. The authors of [22] obtained from (1) the expression for the dimensionless excess chemical potential ϕ of electrons and ions

$$\phi(n_{\mathrm{i}}, T) = 2\pi^{1/2}\gamma^{3/2}(1 - C\lambda\kappa). \tag{2}$$

Equation (1) is obtained for weakly nonideal plasmas, i.e. in the limit $\gamma \ll 1, \lambda\kappa \ll 1$. It is applied for the nonideal region in [22]. The approach is extended to low temperatures here. The equation $(\partial P/\partial V)_T = -(\partial^2 F/\partial V^2)_T = 0$ results in the implicit function $T(n_{\mathrm{e}})$

$$\pi^{1/2}\gamma^{3/2}(1 - 2C\lambda\kappa) = 2 \tag{3}$$

which distinguishes between thermodynamically stable and labile areas. One can say that (3) is a spinodal equation. It has asymptotic $\gamma \approx 1$ (line 1) and $\lambda\kappa = (2C)^{-1}$ (line 2a). Both asymptotics join smoothly in the region of $T_{\mathrm{c}} = 2660$ K. This value of T_{c} follows from both (1) and (2).

2.2. Padé-approximation

The virial expansion, which is similar to (1), is well known in the Debye–Hückel electrolyte theory for charged hard spheres with the diameter a as well. The corresponding expression for the excess chemical potential of the charges of the species i is given by the expression $\mu_{\mathrm{i}}{}^{\mathrm{ex}} = -(e^2\kappa/2kT)(1 - a\kappa)$. The guess is that the virial expansion overestimates repulsion at extrapolating to strong electrolyte, substitute the term $(1 - x)$ by $(1 + x)^{-1}$ and use the approximation; see e.g. [24]

$$\mu_{\mathrm{i}}{}^{\mathrm{ex}} = -(e^2\kappa/2kT)(1 + a\kappa)^{-1}. \tag{4}$$

The approximation

$$\phi(n_{\mathrm{i}}, T) = 2\pi^{1/2}\gamma^{3/2}(1 + C\lambda\kappa)^{-1} \tag{5}$$

is introduced in [22] for nonideal plasma instead of (2) by analogy with (4). $C\lambda$ is an effective repulsion diameter. The authors of [22] obtained $T_{\mathrm{c}} = 10\,640$ K from (5).

Both equations (4) and (5) are Padé-approximations, which are considered to be more reliable for the extrapolation to the nonideal area; diverse Padé-approximations were used in the nonideal plasma theory; see e.g. [23, 24] and references therein. The improved virial expansions were developed. Different other approximations were introduced later on; the T_{c} value range considered is now closer to 10^4 K; see e.g. [23, 24] and references therein. The value $T_{\mathrm{c}} \approx 12\,570$ K is given in [24].

The equilibrium nonideal plasma is treated in [21, 22]. The values of ϕ describe the ionization equilibrium between electrons, ions and atoms in this case. In this paper, we consider nonideal plasma which is not in equilibrium with respect to ionization. So we introduce the Padé-approximation directly for the free energy of electrons and single-charged ions

$$\Delta F_2 = F_{\mathrm{DH}}(1 + 0.75C\lambda\kappa)^{-1}. \tag{6}$$

Equations (1) and (6) coincide with each other when $\gamma \ll 1, \lambda\kappa \ll 1$. The equation $(\partial^2 F/\partial V^2)_T = 0$ for (6) results in the spinodal equation

$$\pi^{1/2}\gamma^{3/2}(1 + 0.25C\lambda\kappa) = 2(1 + 0.75C\lambda\kappa)^3. \tag{7}$$

It has the same asymptotic $\gamma \approx 1$ (line 1) as (3) and a different one $a_0\kappa = (18\pi^2\mathrm{C}^2)^{-1}$ (line 2b), where a_0 is the Bohr radius. Both asymptotics join smoothly in the region of $T_{\mathrm{c}} = 8290$ K.

2.3. van der Waals-like equation

One can rewrite (6) as $F_1 = F_0 + 0.75C\lambda\kappa F_{\rm DH} - F_{\rm DH}$, use direct correspondence with the equation $F_1 = F_0 + (N^2/V)(bT - a)$ and by means of the same procedure as in the van der Waals derivation obtain one more equation of state of nonideal plasma

$$(P + P_{\rm DH})(V - Nb_{\rm DH}) = Nk_BT \tag{8}$$

where $P_{\rm DH} = (1/3)\pi^{1/2}e^3(N/V)^{3/2}(k_BT)^{-1/2}$ is the Debye–Hückel pressure modulo a classical system of charged particles, excluded volume $b_{\rm DH} = \pi\tilde{N}\lambda e^4(k_BT)^{-2}$. The spinodal equation $(\partial P/\partial V)_T = 0$ which follows from (8) is

$$\pi^{1/2}\gamma^{3/2}(1 - 2^{-1}\pi^{1/2}\gamma^{3/2}C\lambda\kappa)^2 = 2 \tag{9}$$

and gives the same first asymptotic $\gamma \approx 1$ (line 1) and one more variant for the second one $\pi^{1/2}\gamma^{3/2}C\lambda\kappa = 2$ (line 2c). Smooth joining of lines 1 and 2c takes place at $T_{\rm c}$ about 10^3 K. The effective repulsion for (9) becomes apparent for the least electron number densities with respect to lines 2a and 2b. The mutual position of curves 2a and 2c corresponds to the idea of the van der Waals derivation.

Line 3 presents a border of degeneracy $\pi^{3/2}\hbar^3 n_{\rm e}/[4(mkT)^{3/2}] = 1$. It is well known that the electron degeneracy provides the thermodynamic stability of electron–ion systems. However it was noticed in 1968 [21] that the thermodynamic stability of nonideal plasmas could be provided by the pair quantum effects in the interaction between free charges. The latter factor is stronger than degeneracy in the $n_{\rm e}$ range considered since line 2a is remarkably higher than line 3. So if one includes degeneracy in the Padé-approximation or van der Waals-like equation in the same way as $\lambda\kappa$ repulsion, it does not influence line 2b or 2c.

For both (1) and (6) and (8) the condition $\gamma \approx 1$ ($\pi^{1/2}\gamma^{3/2} = 2$) corresponds to the change of sign of $(\partial P/\partial V)_T$, i.e. to the loss of the thermodynamic stability at temperatures remarkably less than $T_{\rm c}$. Line 1 bounds from below the area of stability for (1), (6) and (8). As to the scatter between lines 2a, 2b and 2c, it points to the necessity to get some reference points to choose the extrapolation procedure. At the same time lines 2a, 2b and 2c have one and the same common feature: the positive slope of $T(n_{\rm e})$ functions. The reason is that the effective repulsion radius decreases with temperature decrease for all three approximations.

Moreover, independently of approximations used, there are three areas in figure 1. Plasma is ideal or weakly nonideal and thermodynamically stable in area *I* above line 1 where $(\partial P/\partial V)_T < 0$. Recombination takes place in area *I*. Area *I* is slightly shadowed. Plasma is thermodynamically labile (absolutely unstable) in area *II* between lines 1 and 2 where $(\partial P/\partial V)_T > 0$. The condition of thermodynamic stability $(\partial P/\partial V)_T < 0$ is again valid in the shadowed area *III* below line 2. The whole metastability region *III* obtained mainly corresponds to non-degenerate nonideal plasma, where the formally calculated Debye number is remarkably less than 1.

2.4. Rydberg matter at $T = 0$

According to [20] the area of the metastable states is bounded at high densities by losing stability due to radiative and/or Auger recombination. Alternatively one can speak about the dependence of the lifetime τ on the number density $n_{\rm e}$. The function $\tau(n_{\rm e})$ is calculated in [20] for $T = 0$. It is a steep one. We choose the value $n_{\rm e} = 1.5 \times 10^{18}$ cm^{-3} which corresponds to the lifetime $t = 1$ s as a conditional right border of the metastability area (vertical line 5). For comparison the border of the shadow in figure 1 is extended to the value of $n_{\rm e} = 4 \times 10^{18}$ cm^{-3}, which corresponds to the lifetime $\tau = 10^{-3}$ s. One can see that the shift with respect to the vertical 5 is not an important one.

The states to the left of the vertical 5 correspond to the principal quantum numbers greater than 10. Such highly excited states are mostly hydrogen-like. So one can expect that the diagram presented in figure 1 does not depend remarkably on the chemical species.

The metastability in III is of double nature: with respect to (a) radiation and Auger processes and (b) homogeneous nucleation. The conventional heterogeneous nucleation is not the case since the metastable region is an isolated one and the isotherms do not pass smoothly from the metastable states to any stable state [29, 30]. The metastability with respect to collisional recombination is treated in [29].

3. Discussion of experimental data

3.1. Thermodynamically labile plasmas

Several attempts were undertaken to study plasma states in area II experimentally [1] and by simulation [13–15]—points 7, 11 and 12 in figure 1. The placement of the results [1, 13–15] in figure 1 is not an unambiguous procedure. The fact is that the authors of [1] used femtolaser excitation of an ultracold gas and generated collective ultracold nonequilibrium plasma clouds with n_e about 2×10^9 cm^{-3} and temperatures as low as $T_e = 100$ mK for electrons and $T_i = 10$ μK for ions were reported in [1]. The electron state created in [1] is presented in figure 1 by the filled circle 7. The work [1] initiated molecular-dynamics simulation [13–15]. Plasma models are different in [13] and [14, 15] with respect to the effective electron–ion short-range interaction, the authors of [13] use absolute and [14, 15] reduced variables. However the results are almost identical: initial rapid (almost not resolved) heating to the state with the value of γ about unity and then a molecular-dynamics run with a stationary γ or electron temperature. The authors of [4] apply the result to interpret the observation of [1] as well.

The authors of [13–15] are not aware of the absolute instability of plasma states in II and attribute the initial rapid heating completely to the effect of transformation of the potential energy of charged particles into their kinetic energy and buildup of the electron–ion correlations (disorder-induced heating, DIH). It is noticed in [14, 15] that the potential and kinetic energies of charged particles are not in equilibrium with each other in state 7, since the initial coordinates of particles are random as in ideal gas. The DIH is a well-known initial process in molecular dynamics and Monte Carlo simulation [26] and is certainly the case in both simulation [13–15] and experiment [1].

Now the question of relaxation times of the ultracold plasmas is discussed, whether the time of DIH is long enough (a) for plasma to reach a partial thermodynamic equilibrium and (b) for the criterion of thermodynamic instability to be applied. The DIH time takes one–two plasma oscillations [13–15]. On the other hand, the buildup of electron temperature and electron distribution close to the Maxwell one takes only one tenth of a plasma oscillation [27, 28], i.e. much less than the DIH time. So the electron equation of state arises practically from the very beginning of the DIH. Therefore the thermodynamic instability should manifest itself at the same time.

Taking into account the remoteness of points 7, 10 and 11 from line 1, one can suggest that distinction of T_e from T_i does influence the very fact of the thermodynamic instability though the value of $(\partial P/\partial V)_T$ might change with respect to the case $T_e = T_i$. So we think that the relaxation of the initial states 7, 10 and 11 to the region $\gamma \approx 1$ is started by the DIH and then accelerated remarkably by the spinodal decomposition due to the absolute thermodynamic instability resulting in the rapid plasma heating in both [13–15] and [1]. Attention is drawn to the fact that the relaxation processes starting from points 7, 10 and 11 come to an end in the region of the line $\gamma \approx 1$ where the thermodynamic stability is restored.

The molecular-dynamics simulation of the transformation of potential energy into heating of electrons and ions is carried out in [27, 28] as well. The DIH is observed but the plasma states which are simulated correspond to the thermodynamically stable plasmas. Contrary to [13–15] it is possible to obtain different values of γ larger than unity after the relaxation. The relaxation time is remarkably longer than that in [13–15].

3.2. Thermodynamically stable plasmas

The authors [1] extend their measurements outside the area of the absolute instability above area *II* in experiments [2, 3]. The results are presented by open triangles 8 in figure 1. All points 8 are on area *I*. There is no indication of the rapid heating in [2, 3] though initial coordinates of particles are random and not correlated as in [1]. It means that unavoidable DIH does not manifest itself at once if there is no ground for a spinodal decomposition

Xenon plasma is studied in [2, 3]. The open square 9 designates the extreme parameters achieved in [5] for caesium plasma. The authors could not condense Rydberg atoms. They conclude that it is necessary either to increase the density by two orders of magnitude or to lower the temperature to 1 K. It would correspond to border 2.

Line 4 in figure 1 corresponds to the unit value of the Debye number N_{D}. The number of particles in the Debye sphere is less than unity below line 4. One can expect some precursor effects of the plasma nonideality in the border region between lines 1 and 4. Points 8 and 9 are interesting for that reason since there is a problem in estimation of relaxation times for $N_{\mathrm{D}} < 1$ [27, 28].

3.3. Thermodynamically metastable plasmas

Square 6 points to the final state of condensed and cooled caesium microclusters [6, 7] with diameter about 0.5 mm and gas-like density of 10^{18} cm^{-3}. The arrow shows schematically the formation path of microclusters. Note that the stationary states [1] arise as a result of spontaneous internal heating while the microclusters [6, 7] are obtained by means of external forced cooling by liquid nitrogen. The authenticity of the results [6–10] is checked in experiments [12]. Both the existence of stationary microclusters, as well as non-equilibrium states of them are verified by the series of experiments where laser generations are observed from the microclusters [11].

The lifetime of the microclusters is equal to seconds before their radiative deexcitation. This is much longer than the time of establishing equilibrium over any of the internal degrees of freedom. One can thus introduce the notions of temperature, pressure and specific volume, i.e., standard thermodynamic parameters to describe the state of the microclusters. Since the energy is not deposited in the microclusters after their formation during the period of observation, the microcluster state can be related to the metastable states that are considered in thermodynamics. Thus the placement of point 6 in figure 1 is thermodynamically completely correct. Point 6 hits the border region of area *III*, where the thermodynamic stability is restored according to prediction [21, 22]. Hensel told me at SCCS 2005 that he and his colleagues had observed another state which could be placed in area *III* near border 2.

Conclusions

The area of metastability limited by lines 2 and 5 does not contradict the experimental data available [6, 7]. Strongly-coupled non-degenerate electron condensed states are observed in the experiments [6, 7]. The possibility of the existence of thermodynamically labile and metastable states of nonideal plasmas was predicted in the late 1960s [21, 22]. It is shown

that the results of recent experiments and simulation might point to the confirmation of the prediction.

Acknowledgments

This work is partially supported by the RFBR grant 04-02-17065a and the RAS program 'Thermophysics and mechanics of intensive energy impacts'.

References

[1] Killian T C, Kulin S, Bergeson S D, Orozco L A, Orzel C and Rolston S L 1999 *Phys. Rev. Lett.* **83** 4776
[2] Kulin S, Killian T C, Bergeson S D and Rolston S L 2000 *Phys. Rev. Lett.* **85** 318
[3] Killian T C, Lim M J, Kulin S, Dumke R, Bergeson S D and Rolston S L 2001 *Phys. Rev. Lett.* **86** 3759
[4] Killian T C, Ashoka V S, Gupta P, Laha S, Nagel S B, Simien C E, Kulin S, Rolston S L and Bergeson S D 2001 *Phys. Rev. Lett.* **86** 3759
[5] Vitrant G, Raimond J M, Gross M and Haroche S 1982 *J. Phys. B: At. Mol. Opt. Phys.* **15** L49
[6] Aman C, Pettersson J B C and Holmlid L 1990 *Chem. Phys.* **147** 189
[7] Aman C, Pettersson J B C, Lindroth L and Holmlid L 1992 *J. Mater. Res.* **7** 100
[8] Svensson R and Holmlid L 1999 *Phys. Rev. Lett.* **83** 1739
[9] Holmlid L 2001 *Phys. Rev.* A **63** 13817
[10] Holmlid L 2002 *J. Phys.: Condens. Matter* **14** 13469
[11] Holmlid L 2004 *J. Phys. B: At. Mol. Opt. Phys.* **37** 357
[12] Yarygin V I, Sidel'nikov V N, Kasikov I I, Mironov V S and Tulin S M 2003 *JETP Lett.* **77** 280
[13] Mazevet S, Collins L A and Kress J D 2002 *Phys. Rev. Lett.* **88** 55001
[14] Kuzmin S G and O'Neil T M 2002 *Phys. Rev. Lett.* **88** 65003
[15] Kuzmin S G and O'Neil T M 2002 *Phys. Plasmas* **9** 3743
[16] Pohl T, Pattard T and Rost J M 2004 *Phys. Rev. Lett.* **92** 15503
[17] Pohl T, Pattard T and Rost J M 2004 *J. Phys. B: At. Mol. Opt. Phys.* **37** L183
[18] Murillo M S 2001 *Phys. Rev. Lett.* **87** 115003
[19] Bonitz M, Zelener B B, Zelener B V, Manykin E A, Filinov V S and Fortov V E 2004 *JETP* **98** 719
[20] Manykin E A, Ozhovan M I and Poluektov P P 2000 *Chem. Phys. Rep.* **18** 1353
[21] Norman G E and Starostin A N 1968 *High Temp.* **6** 394
[22] Norman G E and Starostin A N 1970 *High Temp.* **8** 381
[23] Kraeft W D, Kremp D, Ebeling W and Röpke R 1996/1986 *Quantum Statistic of Charged Particle Systems* (Berlin/New York: Akademie/Plenum)
[24] Ebeling W and Norman G E 2003 *J. Stat. Phys.* **110** 861
[25] Vedenov A A and Larkin A I 1959 *Zh. Eksp. Teor. Fiz. (USSR)* **36** 1133
[26] Brush S G, Sahlin H L and Teller E 1966 *J. Chem. Phys.* **45** 2102
[27] Morozov I A and Norman G E 2003 *J. Phys. A: Math. Gen.* **36** 6005
[28] Morozov I A and Norman G E 2005 *JETP* **96** 370
[29] Norman G E 2000 *Chem. Phys. Rep.* **18** 1335
[30] Norman G E 2001 *JETP Lett.* **73** 10